A Letters Journal Exploring the Frontiers of Physics

June 2008

EPL, **82** (2008) 68002
doi: 10.1209/0295-5075/82/68002

www.epljournal.org

Phase diagram for a mixture of colloids and polymers with equal size

R. Tuinier[1(a)], P. A. Smith[2], W. C. K. Poon[2], S. U. Egelhaaf[2,3], D. G. A. L. Aarts[4], H. N. W. Lekkerkerker[5] and G. J. Fleer[6]

[1] *Forschungszentrum Jülich, Institut für Festkörperforschung - D-52425 Jülich, Germany*
[2] *SUPA and School of Physics, The University of Edinburgh, Edinburgh - EH9 3JZ, UK*
[3] *Condensed Matter Physics Laboratory, Heinrich-Heine-University - Universitätsstrasse 1, D-40225 Düsseldorf, Germany*
[4] *Department of Chemistry, Physical and Theoretical Chemistry Laboratory, University of Oxford South Parks Road, Oxford OX1 3QZ, UK*
[5] *Van't Hoff Laboratory, Utrecht University - Padualaan 8, 3584 CH Utrecht, The Netherlands*
[6] *Laboratory of Physical Chemistry and Colloid Science, Wageningen University - 6703 HB Wageningen, The Netherlands*

received 29 February 2008; accepted in final form 21 April 2008
published online 29 May 2008

PACS 82.70.Dd – Colloids
PACS 64.60.-i – General studies of phase transitions
PACS 61.25.H- – Macromolecular and polymers solutions; polymer melts

Abstract – We present the phase diagram of a colloid-polymer mixture in which the radius a of the colloidal spheres is approximately the same as the radius R of a polymer coil ($q = R/a \approx 1$). A three-phase coexistence region is experimentally observed, previously only reported for colloid-polymer mixtures with smaller polymer chains ($q \lesssim 0.6$). A recently developed generalized free-volume theory (GFVT) for mixtures of hard spheres and non-adsorbing excluded-volume polymer chains gives a quantitative description of the phase diagram. Monte Carlo simulations also agree well with experiment.

Copyright © EPLA, 2008

Introduction. – The interaction between dispersed colloids can be "tuned" by adding non-adsorbing polymer chains [1]. In a mixture of non-adsorbing polymers and colloids, each particle is surrounded by a layer of solvent depleted of polymer [2–4] because of the loss in configurational entropy of polymer chains near a surface. When the depletion layers of two nearby particles overlap, these particles attract one another [4,5]. This attractive force can be measured using laser tweezers [6].

Depletion forces also modify the phase behaviour of the colloids. A solid knowledge of polymer-induced modifications to the equilibrium phase behaviour of colloids or nanoparticles is fundamental for a better understanding of more complex phenomena such as non-equilibrium aggregation and for the controlled modification of the rheological properties. Furthermore, the behaviour of mixtures containing colloids and polymers of about the same size is relevant for industrial applications, for example high-performance photovoltaic materials (reviewed in [7]). Many of these systems are cast from solutions consisting of mixtures of nanoparticles and conducting polymers with a size ratio of approximately unity.

The equilibrium phase diagram of hard-sphere (HS) colloids is simple: there is only a fluid-solid phase transition when the colloids occupy about half of the volume [8]. The phase behaviour of mixtures of HS colloids and non-adsorbing polymers was first studied experimentally by de Hek and Vrij using silica particles and polystyrene in cyclohexane [9]. They observed a separation into two coexisting colloidal fluid phases at high enough polymer concentrations. Their observations were explained semi-quantitatively using thermodynamic perturbation theory to deal with the effect of an *ideal* polymer on hard spheres at the pair level [10]. The theory predicts fluid-crystal (FC), gas-liquid (GL) and gas-crystal (GC) biphasic regions and a gas-liquid-crystal (GLC) three-phase coexistence *line*. A liquid phase only develops for $q = R/a \gtrsim 0.3$ with q the ratio of the polymer

(a) E-mail: remco.tuinier@googlemail.com

radius of gyration R to the radius of the colloid a. This was first qualitatively confirmed for a charge-stabilized system [11,12] and then FC, GL and GC coexistence were observed in a HS+polymer mixture [13]. No GLC coexistence was reported in these studies.

The dependence of phase diagram topology on the size ratio q was studied in HS-like poly-methylmethacrylate (PMMA) colloids with added flexible polystyrene chains dispersed in *cis*-decalin by Ilett *et al.* [14], who found FC, GL, GC and also GLC coexistence for $q \gtrsim 0.24$. In all cases of coexistence, there was significant polymer partitioning, with more polymer in dilute colloid phases. Polymer partitioning and a three-phase coexistence *region* at large enough q was predicted by free-volume theory (FVT) [15], and confirmed by subsequent computer simulations [16,17]. GLC coexistence has also been observed in aqueous colloids and added polysaccharides [18,19] with $q \approx 0.25$ and ≈ 0.6.

To date, GLC triple coexistence has only been reported for $0.24 \lesssim q < 0.65$. GLC for larger q values is difficult to realize experimentally, as this requires relatively large polymers and small colloids which, moreover, should be nearly monodisperse. In most high-q experiments reported in the literature the particles were so polydisperse that crystallization proved impossible [20]. Thus, for example, the work of De Hoog and Lekkerkerker at $q \approx 1$ [21] and of Zhang and Van Duijneveldt [22] at $q \approx 5$ only reported GL coexistence. In this paper we provide an experimental example for $q \approx 1$ where the particles are monodisperse enough to show crystallization and, consequently, GLC triple coexistence.

There are significant quantitative discrepancies between FVT and experiments, especially for $q > 0.5$. At $q = 0.57$, FVT underestimates overall phase boundary positions by a factor of 2 in polymer concentration and overestimates the size of the GLC coexistence region considerably [14]. More dramatically, FVT underestimates the polymer concentration in the colloidal liquid at triple coexistence by two orders of magnitude [23]. For higher q, the deviations between FVT and experiment are even worse [21,22].

Two of us have recently proposed a generalized free-volume theory (GFVT, generalized FVT) for the phase behaviour of colloid-polymer mixtures [24]. For small q (the so-called *colloid limit*) its predictions are close to those of FVT, but for higher q it takes into account the compression of the depletion layers in semidilute solutions and nonideal contributions to the osmotic pressure. In the so-called *protein limit* ($q \gg 1$) a simple scaling of the binodal polymer concentrations with q is found; these predictions were tested using data from computer simulations [25] and found to agree. Here we confront this theory with a full experimental phase diagram of a colloid-polymer mixture with $q \approx 1$ and nearly monodisperse particles. The $q \approx 1$ case is particularly interesting compared to either $q \ll 1$ or $q \gg 1$. In the latter situations, the smaller component can be treated perturbatively, starting from a theory of a system consisting of just the larger component. In contrast, a perturbative approach is inappropriate for $q \approx 1$.

The experimental phase diagram shows all the regions predicted by perturbation [10] and free-volume [15] theories, including GLC triple coexistence. As will be shown, GFVT is able to give not only a qualitative but also a quantitative account of our observations.

Materials and methods. – Sterically stabilized PMMA colloids with radius $a = 130 \pm 2\,\mathrm{nm}$ (from static light scattering) were synthesized according to literature procedures [26]. The colloid volume fraction η was calibrated by measuring the fraction of colloidal crystals in the fluid-crystal coexistence region, which varies linearly from 0% to 100% in the interval $0.494 < \eta < 0.545$. From the speed of the crystallization of the pure HS colloids, we estimate that the polydispersity is smaller than 5%. We used linear polystyrene (Polymer Laboratories) with molar weight $M_\mathrm{w} = 15.4 \times 10^6\,\mathrm{g/mol}$. The solvent was a mixture of *cis*-decalin and tetralin to match the refractive index of the colloids. Samples at various colloid volume fractions η and polymer concentrations ϕ were well mixed and then kept in a water bath at 16 °C for observations. We refer to the polymer concentration in terms of an effective concentration ϕ/ϕ^*, where ϕ^* is the effective polymer concentration at overlap.

The behaviour of polystyrene in *cis*-decalin has been documented in detail by Berry [27]. At the theta temperature, $13\,^\circ\mathrm{C} \equiv 286\,\mathrm{K} = T_\theta$, the radius of gyration of the polymer is given by

$$R(T_\theta) = 0.028\,\mathrm{nm}\sqrt{M_w/\mathrm{g\,mol^{-1}}}. \qquad (1)$$

Berry characterized the chain non-ideality at temperature $T > T_\theta$ by a dimensionless parameter z, which obeys

$$z = 0.00975\sqrt{M_w/\mathrm{g\,mol^{-1}}}\,(1 - T_\theta/T)\,, \qquad (2)$$

where the temperatures are in kelvin. Figure 12 in Berry's paper gives R as a function of z and allows us to estimate R of polystyrene of arbitrary M_w in *cis*-decalin at any T. In this way we find that in *cis*-decalin at 16 °C our polymer has $z = 0.5$ and a swollen size of $R = 125\,\mathrm{nm}$. There is little quantitative information on polystyrene in mixtures of *cis*-decalin and tetralin or in pure tetralin. It has, however, been reported that the addition of tetralin to a cyclohexane solution of polystyrene (at the latter's theta temperature, 34 °C) has little effect on the polymer [28]. We may thus expect that tetralin does also not change the polymer size R very much for polystyrene dissolved in *cis*-decalin just above this solvent's theta temperature. Therefore, we estimate the size ratio of our system to be $q \approx 125/130 \approx 1$. The overlap concentration, calculated from a mass M_w/N_av in a volume $4\pi R^3/3$, is found to be $3.1\,\mathrm{g}/\ell$.

Results and discussion. – The experimentally observed phases are represented as a function of sample

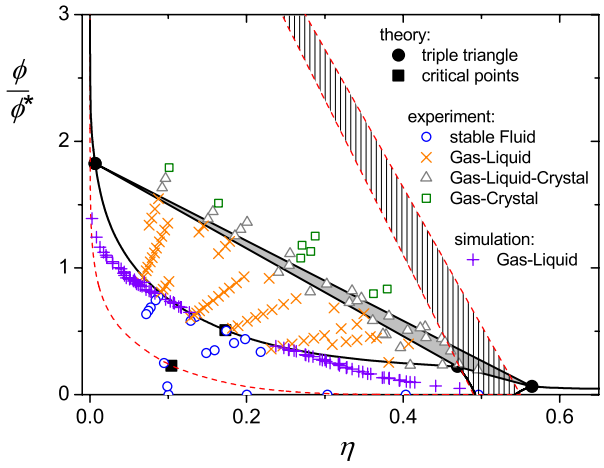

Fig. 1: Phase diagram of a colloid-polymer mixture with $q \approx 1$. Experimental observations are indicated by open symbols and crosses as listed within the figure. The theoretical triple triangle according to FVT [15] (dashed lines) and GFVT [24] (solid lines) are also shown; filled circles correspond to the composition of coexisting GLC phases at the triple point predicted by GFVT. The theoretical FC, GL and GC binodals are indicated as the dashed (FVT) and solid (GFVT) curves, with the theoretical predictions for the critical points represented by filled squares. The pluses correspond to Monte Carlo simulation results [25] for the gas-liquid binodal of hard spheres and self-avoiding polymer chains with a size ratio $q = 1.05$.

composition, *i.e.*, colloid volume fraction η and effective polymer concentration ϕ/ϕ^*, in fig. 1. Below $\eta = 0.5$ a stable one-phase fluid (circles) is found for low polymer concentrations. At higher polymer concentrations GL coexistence (crosses) is observed, as already found in many experimental systems with $q \geqslant 1$ [21,22,29–32]. Further increase of ϕ/ϕ^* results in three-phase coexistence (triangles), previously experimentally found only for $0.24 \lesssim q \lesssim 0.6$ [14,18,19]. At polymer concentrations beyond triple coexistence we observed GC coexistence (squares). At higher η and ϕ/ϕ^* outside the range of equilibrium data points shown in fig. 1, we observed a range of non-equilibrium behaviour. The non-equilibrium data are not shown, because the discussion of such behaviour is outside the scope of the present work.

We compare the experimentally observed phase diagram with FVT [15] and GFVT [24]. As shown by the dashed triple triangle in fig. 1, FVT greatly overestimates the GLC triple region (vertically hatched area). The gas side of this triple triangle (outside the scale of fig. 1) is situated at $\phi/\phi^* = 6$ at very low η. The GL binodal according to FVT (dashed curve with the critical point indicated as the square) lies entirely in the experimental one-phase fluid region, and thus underestimates the experimental binodal.

Previously, Aarts *et al.* [33] incorporated excluded-volume interactions between polymer segments into FVT by using renormalization group (RG) theoretical results [34]. This gives a better description of the phase diagram at large q-values as compared to original FVT [15] but it still overestimates the polymer concentrations at which demixing takes place due to a too small RG correlation length (see fig. 19.10 in ref. [34]).

GFVT [24] describes the semidilute correlation length correctly. This model accounts for the crossover of the depletion thickness δ (next to a flat plate) from a value of order R in dilute polymer solutions to a value $\xi \sim \varphi^{-\gamma}$ [2] in semidilute solutions [35], and for the crossover of the osmotic pressure from the ideal (Van't Hoff) law $\Pi = \varphi/N$ to the semidilute (De Gennes) limit $\Pi \sim \xi^{-3} \sim \varphi^{3\gamma}$ [2,35], where φ is the polymer volume fraction in the free volume (or in an external reservoir). For excluded-volume chains the De Gennes exponent γ equals 0.77. Also the numerical prefactors of these semidilute scaling laws could be established [35], so that quantitative theory becomes possible. Throughout we use dimensionless quantities (all lengths in units of the Kuhn length l, Π in units of kT/l^3, etc.).

In the spirit of original FVT we consider in GFVT the semi-grand potential Ω of a colloid-polymer mixture with volume V in equilibrium with an external reservoir containing only the polymer solution. The colloids cannot enter the reservoir. Unlike in FVT we account for the solvent as a separate component. We use the normalized grand potential $\omega = \Omega v/V$, with the colloid volume $v = 4\pi a^3/3$. The fugacity of the polymer chains in the system is set by the polymer volume fraction φ in the reservoir. The polymer concentration ϕ in the system is related to φ through $\phi = \alpha\varphi$, where α (eq. (4)) is the free volume fraction in the system. We define the reduced external concentration y by $y = \varphi/\varphi^*$, where $\varphi^* = \phi^*$ is the overlap concentration.

The grand potential ω is separated in a hard-sphere (HS) part ω_0 (treated just as in [33]) and a polymer contribution ω_p. Without approximation it follows for ω_p:

$$\omega_p = -\int_0^y \alpha(\partial \Pi v/\partial y)\mathrm{d}y. \tag{3}$$

For the free volume fraction α we use the standard scaled-particle result [15,33]:

$$\alpha = (1-\eta)\exp(-Af - Bf^2 - Cf^3), \tag{4}$$

where $f = \eta/(1-\eta)$, $A = (1+q_s)^3 - 1$, $B = 3q_s^2(q_s + 3/2)$, and $C = 3q_s^3$. Here $q_s = \delta_s/a$, with δ_s the thickness of the depletion zone around a colloidal sphere with radius a. Curvature effects are included through $q_s = 0.815(\delta/a)^{0.88}$, which is an excellent approximation [36] to the more complicated expression given by Aarts *et al.* [33].

For δ and Πv we use recent results, which have been shown to be in excellent agreement with simulations and with experiment [35]. We find

$$q_s = 0.865\left(q^{-2} + 3.95Y^{2\gamma}\right)^{-0.44}, \tag{5}$$

$$\partial \Pi v/\partial Y = q^{-1/\nu} + 3.77Y^{3\gamma-1}, \tag{6}$$

where the parameter Y is defined by

$$Y = yq^{-1/\gamma}. \tag{7}$$

The parameter ν in eq. (6) is the Flory exponent, which is directly related to the De Gennes exponent γ through $1/\nu + 1/\gamma = 3$.

The parameter Y is a convenient normalized polymer concentration which has the important property that it becomes independent of the size ratio q in the protein limit (high q) [24], where the polymer concentrations along the binodals are in the semidilute regime. Then $\delta = \xi \sim \varphi^{-\gamma}$ [2], which does not depend on R. Hence, δ/a does not depend on $q = R/a$, and $q_s = 0.815(\delta/a)^{0.88}$ reaches a constant (q-independent) level. According to eq. (5), $q_s = 0.47Y^{-0.68}$ in the protein limit, so also Y becomes independent of q. In the colloid limit (small q) the binodal polymer concentrations are in the dilute regime, and $q_s = 0.865q^{0.88}$ does depend on q. In this limit Y is a function of q as well [36].

According to eq. (7), $y = Yq^{1/\gamma}$ diverges as $q^{1/\gamma} = q^{1.3}$ in the protein limit, where Y is constant. This predicted $q^{1.3}$ scaling [24] of protein-limit binodals is corroborated by simulations [25]. In the colloid limit, where Y depends on q, this scaling does not apply. Analytical approximations for $Y^{\rm cp}$ (critical points) and $Y^{\rm tp}$ (triple points) as a function of q are available [36].

The above equations allow us to calculate the two parameters that represent the new ingredients in GFVT: the effective size ratio $q_s = \delta_s/a$ and the osmotic pressure Π, which only occurs as the product Πv; it is the osmotic work to insert a particle (without depletion layer) into the polymer solution. Plots of q_s and Πv as a function of $y = \varphi/\varphi^*$ are given in fig. 2, for three values of q: 0.4 (representative for the colloid limit), 1 (relevant for the results in fig. 1), and 5 (protein limit). The effective size ratio crosses over from $q_s = 0.865\ q^{0.88}$ (close to but smaller than q) at low y towards $0.47Y^{-0.68} = 0.47y^{-0.68}q^{0.88}$; the exponent for y is smaller than $\gamma = 0.77$ because of curvature effects. The osmotic pressure changes from the ideal law $\Pi v = Yq^{-1/\nu} = yq^{-3}$ towards the semidilute (De Gennes) behaviour $\Pi v = 1.62Y^{3\gamma} = 1.62y^{3\gamma}q^{-3}$.

A very important feature of fig. 2 is that the semidilute power law sections are horizontally shifted with respect to each other by an amount $1.3\log(q)$. Hence, when the figure is replotted with Y instead of y along the abscissa axis, these semidilute branches collapse onto a single curve (not shown), because Y in the semidilute limit (corresponding to the protein limit) does not depend on q. The vertical shift in fig. 2 is $0.88\log(q)$ for q_s and $3\log(q)$ for Πv over the whole range of y: plots of $q_s q^{-0.88}$ and $\Pi v q^3$ as a function of y would give universal curves.

Equations (4), (5) and (6) provide the ingredients for ω_p in eq. (3). The latter equation is now used with y replaced by Y. Standard thermodynamics enables the calculation of the full phase diagram from $\omega = \omega_0 + \omega_p$ and its derivatives with respect to η. For these derivatives explicit analytical expressions are available [36].

We plot the GFVT predictions for mixtures of HS and polymer chains with excluded-volume interaction and $q = 1$ in fig. 1 as the solid curves for the binodal and solid lines for the triple triangle. The filled circles correspond to the compositions of coexisting GLC samples at the triple point, while the filled square represents the critical point. It is evident that GFVT gives an excellent account of the GL binodal, as well as good agreement with the GLC three-phase coexistence.

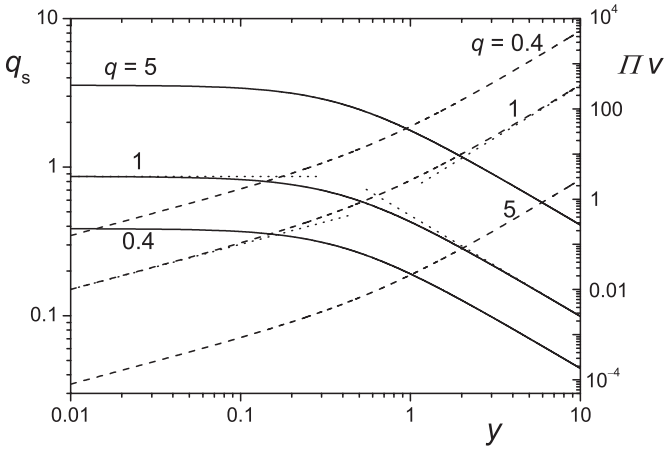

Fig. 2: Dependence of the effective size ratio q_s (left axis; solid curves) and insertion work Πv (right axis; dashed curves) on the effective (external) polymer concentration y, for $q = 0.4$, 1, and 5. For $q = 1$ the dilute and semidilute limits are indicated as the dotted lines.

In fig. 1 we inserted GL binodal points (pluses) from Monte Carlo simulations for hard spheres and self-avoiding polymer chains [25] with a size ratio $q = 1.05$. The agreement of these simulations with experiment and with the GFVT binodal for $q = 1$ is quite good. It is clear that properly accounting for excluded-volume interactions between polymer segments, as in GFVT, gives a better description of the GL simulations. Simulation data of three-phase equilibria for HS plus interacting polymer chains are not yet available.

Further effects might be responsible for the minor quantitative discrepancies. The GFVT computations (and simulations) are for a good solvent, whereas the polymer in the experiments is probably in a moderately good solvent, in between the theta and athermal limits. The numerical constants in GFVT (see eqs. (5) and (6)) were obtained from RG theory and simulations, and might be slightly different for real systems; in principle these constants are available from carefully designed experiments [35]. Moreover, the particles in any real experiment have finite polydispersity. The effect of particle polydispersity on the phase behaviour of mixtures of hard spheres and ideal polymers at low size ratios has been explored ($q < 0.5$) [37]. Even modest polydispersities ($< 10\%$) can significantly change the phase diagram topology by introducing a host of new, multiphasic equilibria involving multiple solid phases[1]. Fasolo and Sollich [37] used original FVT in

[1]In practice, such multiphasic equilibria may show up as kinetic effects preventing the system reaching equilibrium. The non-equilibrium behaviour we observed at high (η, ϕ), already mentioned above, may partly be due to this effect.

their treatment of particle polydispersity. It should be possible to combine their approach with GFVT to predict how particle polydispersity affects the phase behaviour at $q \approx 1$.

Finally, we note that the thermodynamic concepts of original FVT to describe polymer-colloid phase diagrams seem to be sound. The only new aspect of GFVT is to include the correct dependence of the depletion thickness and osmotic pressure on polymer concentration. With this modification the application of (G)FVT to more complex systems, including for instance charged colloids [38], seems possible. GFVT is valid for any size ratio q and for any polymer concentration up to and including the semidilute regime. It breaks down in the concentrated regime, but in this regime experiments are very difficult, because of high viscosity and extremely slow equilibration. In practice, GFVT would describe most experimentally accessible binodal curves.

Conclusions. – In this letter we have described the phase behaviour of a mixture of hard-sphere colloids and non-ideal polymer chains of about the same size. For the first time a three-phase coexistence region is experimentally observed for a size ratio $q > 0.6$. Generalized free-volume theory (GFVT), which accounts for excluded-volume interactions, correctly predicts the experimental phase diagram, in particular the gas-liquid (GL) binodal and the gas-liquid-crystal three-phase region (GLC). It also agrees well with Monte Carlo simulations for mixtures of hard spheres and self-avoiding polymer chains.

* * *

We thank A. B. Schofield for synthesizing the PMMA particles, and P. G. Bolhuis for sending us his MC data. Part of this project has been supported by the European Commission under the 6th Framework Program through integrating and strengthening the European Research Area. Contract: SoftComp, NoE/NMP3-CT-2004-502235.

REFERENCES

[1] Poon W. C. K., *J. Phys: Condens. Matter*, **14** (2002) R859.
[2] de Gennes P.-G., *Scaling Concepts in Polymer Physics* (Cornell University Press, Ithaca) 1979.
[3] Fleer G. J., Cohen Stuart M. A., Scheutjens J. M. H. M., Cosgrove T. and Vincent B., *Polymers at Interfaces* (Chapman and Hall, London) 1993.
[4] Asakura S. and Oosawa F., *J. Chem. Phys.*, **22** (1954) 1255.
[5] Vrij A., *Pure Appl. Chem.*, **48** (1976) 471.
[6] Verma R., Crocker J. C., Lubensky T. C. and Yodh A. G., *Macromolecules*, **33** (2000) 177.
[7] Saunders B. R. and Turner M. L., *Adv. Colloid Interface Sci.*, **138** (2008) 1.
[8] Pusey P. N. and van Megen W., *Nature*, **320** (1986) 340.
[9] de Hek H. and Vrij A., *J. Colloid Interface Sci.*, **84** (1981) 409.
[10] Gast A. P., Hall C. K. and Russel W. B., *J. Colloid Interface Sci.*, **96** (1983) 251.
[11] Sperry P. R., Hopfenberg H. B. and Thomas N. L., *J. Colloid Interface Sci.*, **82** (1981) 62.
[12] Sperry P. R., *J. Colloid Interface Sci.*, **87** (1982) 365; **99** (1984) 97.
[13] Vincent B., Edwards J., Emmett S. and Croot R., *Colloids Surf.*, **31** (1988) 267.
[14] Ilett S. M., Orrock A., Poon W. C. K. and Pusey P. N., *Phys. Rev. E*, **51** (1995) 1344.
[15] Lekkerkerker H. N. W., Poon W. C. K., Pusey P. N., Stroobants A. and Warren P. B., *Europhys. Lett.*, **20** (1992) 559.
[16] Meijer E. J. and Frenkel D., *J. Chem. Phys.*, **100** (1994) 6873.
[17] Dijkstra M., van Roij R., Roth R. and Fortini A., *Phys. Rev. E*, **73** (2006) 041404.
[18] Leal-Calderon F., Bibette J. and Biais J., *Europhys. Lett.*, **23** (1993) 653.
[19] Faers M. A. and Luckham P. F., *Langmuir*, **15** (1997) 2922.
[20] Bolhuis P. G. and Kofke D. A., *Phys. Rev. E*, **54** (1996) 634.
[21] de Hoog E. H. A. and Lekkerkerker H. N. W., *J. Phys. Chem. B*, **103** (1999) 5274.
[22] Zhang Z. X. and van Duijneveldt J. S., *Langmuir*, **22** (2006) 63.
[23] Moussaïd A., Poon W. C. K., Pusey P. N. and Soliva M. F., *Phys. Rev. Lett.*, **82** (1999) 225.
[24] Fleer G. J. and Tuinier R., *Phys. Rev. E*, **76** (2007) 041802.
[25] Bolhuis P. G. *et al.*, *Phys. Rev. Lett.*, **89** (2002) 128302; **90** (2003) 068304.
[26] Antl L., Hill R. D., Ottewil R. H., Owens S. M., Papworth S. and Waters J. A., *Colloids Surf.*, **17** (1986) 67.
[27] Berry C. G., *J. Chem. Phys.*, **44** (1966) 329.
[28] Abdel-Azim A.-A. and Huglin M. B., *Europhys. Polym. J.*, **20** (1984) 329.
[29] Bodnár I., Dhont J. K. G. and Lekkerkerker H. N. W., *J. Phys. Chem.*, **100** (1994) 19614.
[30] Tuinier R., Dhont J. K. G. and de Kruif C. G., *Langmuir*, **16** (2000) 1497.
[31] Ramakrishnan S., Fuchs M., Schweizer K. S. and Zukoski C. F., *J. Chem. Phys.*, **116** (2002) 2201.
[32] Hennequin Y., Evens M., Quezada Angulo C. M. and van Duijneveldt J. S., *J. Chem. Phys.*, **123** (2005) 054906.
[33] Aarts D. G. A. L., Tuinier R. and Lekkerkerker H. N. W., *J. Phys: Condens. Matter*, **14** (2002) 7551.
[34] L. Schäfer., *Excluded Volume Effects in Polymer Solutions* (Springer-Verlag, Heidelberg) 1999.
[35] Fleer G. J., Skvortsov A. M. and Tuinier R., *Macromol. Theory Sim.*, **16** (2007) 531.
[36] Fleer G. J. and Tuinier R., submitted to *Adv. Colloid Interface Sci.* (2008).
[37] Fasolo M. and Sollich P., *J. Chem. Phys.*, **122** (2005) 074904.
[38] Fortini A., Dijkstra M. and Tuinier R., *J. Phys: Condens. Matter*, **17** (2005) 7783.